

30 Mar 2001, 4:30 pm - 6:30 pm

## Effect of the Non-Linear Behavior of Pile Material on the Response of Laterally Loaded Piles

Mohamed Ashour  
*University of Nevada, Reno, NV*

Gary Norris  
*University of Nevada, Reno, NV*

Anooshirvan Shamsabadi  
*California Department of Transportation, Sacramento, CA*

Follow this and additional works at: <https://scholarsmine.mst.edu/icrageesd>



Part of the [Geotechnical Engineering Commons](#)

### Recommended Citation

Ashour, Mohamed; Norris, Gary; and Shamsabadi, Anooshirvan, "Effect of the Non-Linear Behavior of Pile Material on the Response of Laterally Loaded Piles" (2001). *International Conferences on Recent Advances in Geotechnical Earthquake Engineering and Soil Dynamics*. 15.

<https://scholarsmine.mst.edu/icrageesd/04icrageesd/session06/15>



This work is licensed under a [Creative Commons Attribution-Noncommercial-No Derivative Works 4.0 License](#).

This Article - Conference proceedings is brought to you for free and open access by Scholars' Mine. It has been accepted for inclusion in International Conferences on Recent Advances in Geotechnical Earthquake Engineering and Soil Dynamics by an authorized administrator of Scholars' Mine. This work is protected by U. S. Copyright Law. Unauthorized use including reproduction for redistribution requires the permission of the copyright holder. For more information, please contact [scholarsmine@mst.edu](mailto:scholarsmine@mst.edu).

# EFFECT OF THE NON-LINEAR BEHAVIOR OF PILE MATERIAL ON THE RESPONSE OF Laterally LOADED PILES

**Mohamed Ashour**  
University of Nevada, Reno  
Reno, Nevada-USA-89557

**Gary Norris**  
University of Nevada, Reno  
Reno, Nevada-USA-89557

**Anooshirvan Shamsabadi**  
California Dept. of Transportation  
Sacramento, California-USA-94274

## ABSTRACT

The main purpose of this study is to assess the lateral response of piles/shafts and the p-y curves for different soil-pile combinations while introducing the effect of the moment-curvature ( $M - \Phi$ ) relationship of the pile into the soil-pile interaction. Therefore, the equilibrium among soil reaction, pile deflection pattern, pile-head load, and flexural stiffness distribution should be satisfied at any level of loading. The influence of the nonlinear behavior of the pile/drilled shaft material on the nature of the associated p-y curve is presented through strain wedge (SW) model analysis. The SW model allows the assessment of the (soil-pile) modulus of subgrade reaction (i.e. the p-y curve) based on soil and pile properties which includes the pile bending stiffness. Therefore, the assessed modulus of subgrade reaction will be affected by changes in the bending stiffness of the pile or drilled shaft at any pile cross section (via the  $M-\Phi$  relationship). The reduction in pile bending stiffness will affect the pile-head stiffness under varying static or dynamic loading.

## INTRODUCTION

Behavior of piles under lateral loading is basically influenced by the properties of both the soil and pile (pile material and shape). The nonlinear modeling of pile material, whether it is steel and/or concrete, should be employed in order to predict the value of the lateral load and the realistic associated bending moment and pile deflection especially at large values of pile-head deflection and the onset of pile material failure. It is known that the variation in the bending stiffness ( $EI$ ) of a laterally loaded pile is a function of the bending moment distribution along the pile (moment-curvature,  $M-\Phi$ , relationship) as seen in Fig. 1. Consequently, some of the pile cross sections which are subjected to high bending moment experience a reduction in bending stiffness and softer interaction with the surrounding soil. Such behavior is observed with drilled shafts and steel piles at advanced levels of loading and has an impact on the lateral response and capacity of the loaded pile. The pile bending stiffnesses along the deflected pile change with the level of loading, the  $M-\Phi$  relationship of the pile material, and the soil reaction which affects the pattern of pile deflection. Therefore, the equilibrium among the distributions of pile deflection, bending moment, bending stiffness, and soil reaction along the pile should be maintained.

The Strain Wedge (SW) model approach, which has been developed to predict the response of a flexible pile under lateral loading, has the capability to carry out such an analysis.

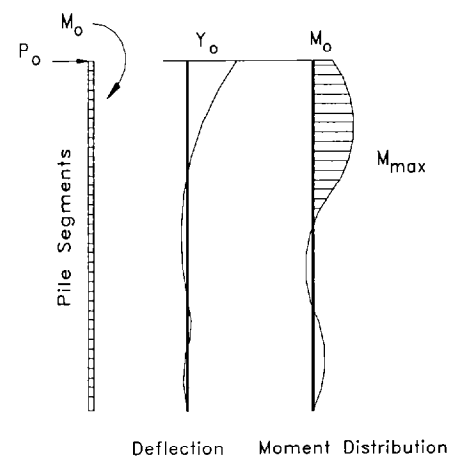


*Fig. 1. Behavior of a laterally loaded pile divided into segments*

The SW model allows the assessment of the (soil-pile) modulus of subgrade reaction (i.e. the secant slope of the p-y curve) based on soil and pile properties which includes the pile bending stiffness. Therefore, the assessed modulus of subgrade reaction will be affected by the changes in the bending stiffness of the pile at any pile cross section, particularly when the drop in bending stiffness is significant.

The currently available technique (Reese 1984), which employs

the Matlock-Reese p-y curves, requires separate evaluation of the M- $\Phi$  relationship of the pile cross section and then adoption of a reduced bending stiffness ( $EI_r$ ) to replace the original pile bending stiffness ( $EI$ ). The suggested procedure utilizes this reduced bending stiffness ( $EI_r$ ) over the full length of the pile at all levels of loading. Assuming a reasonable reduction in bending stiffness, particularly with drilled shafts, is a critical matter that requires guidance from the literature which has only limited experimental data. At the same time, the use of one constant reduced bending stiffness for the pile/shaft does not reflect the real progressive deformations and forces associated with the steps of lateral loading. However, this technique may work quite well with the steel H-pile which approximately fails once the pile flange reaches the yielding stage (occurs rapidly). In general, the response of the pile/drilled shaft (pile-head load vs. deflection, and pile-head load vs. maximum moment) is assessed based on a constant bending stiffness ( $EI_r$ ) and is truncated at the ultimate bending moment of the original pile/drilled shaft cross section. The moment-curvature relationship, and thus the maximum bending moment carried by the pile cross section should be evaluated first.

Reese and Wang (1994) enhanced the technique presented above by computing the bending moment distribution along the pile and the associated value of  $EI$  at each increment of loading. Reese and Wang (1994) concluded that the bending moment along the pile does not depend strongly on structural characteristics and that the moment differences due to  $EI$  variations are small. It should be noted that the effect of the varying  $EI$  on the bending moment values along the drilled shaft was not obvious because the  $EI$  of the drilled shaft had no effect on the p-y curves (i.e. modulus of subgrade reaction) employed in their procedure. Therefore, it was recommended that a single value of  $EI$  of the cracked section (constant value) be used for the upper portion of the pile throughout the analysis. Contrary to Reese and Wang's assumption, the variation in the value of  $EI$  has a significant effect on the nature of the p-y curve and modulus of subgrade reaction [Ashour and Norris (2000); Yoshida and Yoshinaka (1972); and Vesic (1961)] specially in the case of drilled shafts.

## NUMERICAL MODELS OF PILE/DRILLED SHAFT MATERIALS

In order to incorporate the effect of material nonlinearity, numerical material models should be employed in the analysis of the laterally loaded pile/shaft. A unified stress-strain approach for confined concrete has been employed with the reinforced concrete pile as well as a steel pipe pile filled with concrete. In addition, steel is modeled using an elastic-perfectly plastic uniaxial stress-strain relationship commonly used to describe steel behavior.

### Material Modeling of Concrete Strength and Failure Criteria

Based upon a unified stress-strain approach for the confined concrete proposed by Mander et al. (1988), a concrete model is employed with circular and rectangular concrete sections. The proposed model, which is shown in Fig. 2, has been employed

for monotonic loading at a slow strain rate.

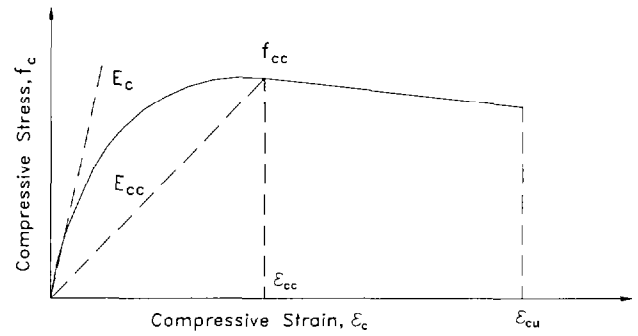


Fig. 2. Stress-strain model for confined concrete in compression (Mander et al. 1988).

In order to determine the compressive strength of the confined concrete ( $f_{cc}$ ), a constitutive model (Mander et al. 1988) is directly related to the effective confining stress ( $f_l$ ) that can be developed at the yield of the transverse reinforcement.

$$f_{cc} = f_{co} \left[ -1.254 + 2.254 \left( 1 + \frac{7.94 f_l}{f_{co}} \right)^{0.5} - \frac{2f_l}{f_{co}} \right] \quad (1)$$

The longitudinal compressive concrete stress  $f_c$  is given by

$$f_c = \frac{f_{cc} x r}{r - 1 + x^r} \quad (2)$$

$$\epsilon_{cc} = \epsilon_{co} \left[ 1 + 5 \left( \frac{f_{cc}}{f_{co}} - 1 \right) \right] \quad (3)$$

where  $f_{cc}$  symbolizes the compressive strength of confined concrete and  $x = \epsilon_c / \epsilon_{cc}$ .  $\epsilon_c$  indicates the axial compressive strain of concrete.  $\epsilon_{cc}$  is the axial strain at the peak stress.  $f_{co}$  and  $\epsilon_{co}$  represent the unconfined (uniaxial) concrete strength and the corresponding strain, respectively.

$$r = \frac{E_c}{E_c - E_{sec}} \quad \text{where} \quad E_c = 57,000 (f_{co})^{0.5} \quad (psi)$$

$$\text{and} \quad E_{sec} = \frac{f_{cc}}{\epsilon_{cc}} \quad (4)$$

Generally,  $\epsilon_{co}$  can be assumed equal to 0.002, and  $E_c$  is the initial

modulus of elasticity of the concrete under slowly applied compression load.

As mentioned by Paulay and Priestly (1992), the strain at peak stress given by Eqn. 3 does not represent the maximum useful strain for design purposes. The concrete strain limits occur when transverse confining steel fractures. A conservative estimate for ultimate compression strain ( $\epsilon_{cu}$ ) is given by

$$\epsilon_{cu} = 0.004 + \frac{1.4 \rho_s f_{yh} \epsilon_{sm}}{f_{cc}} \quad (5)$$

where  $\epsilon_{sm}$  is the steel strain at maximum tensile stress (ranges from 0.1 to 0.15), and  $\rho_s$  is the volume ratio of confining steel. Typical values for  $\epsilon_{cu}$  range from 0.012 to 0.05.  $f_{yh}$  represents the yield stress of the transverse reinforcement.

Although concrete tensile strength is traditionally ignored in flexural strength calculation, it will be more realistic to consider it here in the calculation due to the effect of concrete confinement. As suggested by Mander et al. (1988), a linear stress-strain relationship in tension is assumed up to the tensile strength ( $f_{tu}$ ). The tensile stress is given by

$$f_t = E_c \epsilon_c \quad \text{for } f_t \leq f_{tu} \quad (6)$$

$$\epsilon_{tu} = \frac{f_{tu}}{E_c} \quad \text{and} \quad f_{tu} = 9 (f_{co})^{0.5} \quad (psi) \quad (7)$$

If tensile strain  $\epsilon_t$  is greater than the ultimate tensile strain ( $\epsilon_{tu}$ ),  $f_t$  is assumed to be equal to zero.

**Material Modeling of Steel Strength and Failure Criteria**

There are different numerical models to represent the stress-strain relationship of steel. The model employed for steel in this study is linearly elastic-perfectly plastic, as shown in Fig. 3. The complexity of using this numerical model occurs in the plastic portion of the model which does not include any strain hardening (perfectly plastic).

Elastic behavior of the steel occurs where the strain is less than the yield strain  $\epsilon_y$ .

$$\epsilon_y = \frac{f_y}{E_{s0}} \quad (8)$$

where  $f_y$  is the yield stress of steel, and  $E_{s0}$  is the elastic Young's

modulus of steel which is equal to  $2 \times 10^5$  MPa.

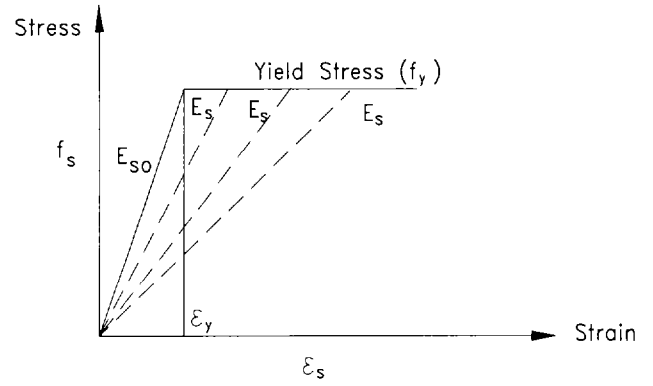


Fig. 3. Elastic-perfectly plastic model for steel.

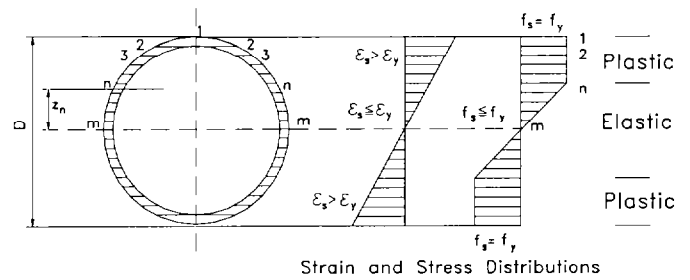


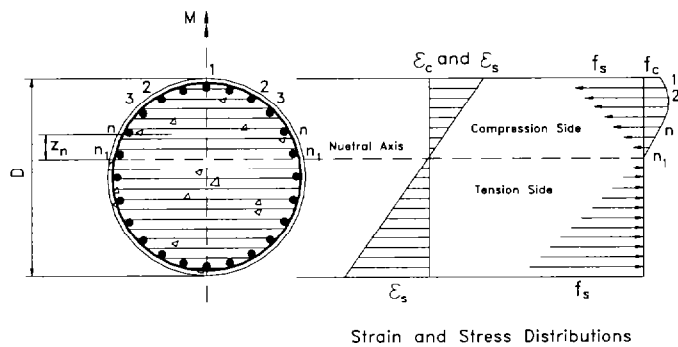
Fig. 4. Behavior of a steel cross section in the elastic-plastic stage.

When the value of steel stress ( $f_s$ ) at any point on the cross section reaches the yield stress, the Young's modulus diminishes to values less than  $E_{s0}$  (of the elastic zone). The initial yielding takes place when the stress at the farthest point from the neutral axis on the steel cross section (strip 1) becomes equal to the yield stress ( $f_y$ ), as shown in Fig. 4.

Initial yielding indicates the beginning of the elastic-plastic response of the steel section and the accompanying reduction in bending stiffness ( $EI$ ). By increasing the load, other internal points on the cross section will progressively respond in a plastic fashion at a constant stress ( $f_y$ ), as seen in Fig. 4. Once all points on the steel section satisfy a normal stress ( $f_s$ ) equal to the yield stress ( $f_y$ ) or a strain value larger than the yield strain ( $\epsilon_y$ ), the steel section responds as a plastic hinge with an ultimate plastic moment ( $M_p$ ) indicating the complete yielding of the steel section. However, this does not indicate the failure of the pile, but effectively slows the growth in pile capacity.

Figure 5 shows the stress and strain distribution in a R/C cross section. Both nonlinear models of steel and concrete are employed under a linear strain distribution over the whole shaft cross section. However, the area and bending stiffness of the R/C section gradually diminishes due to the increasing tensile stress in the concrete.

Fig. 5. Behavior of reinforced concrete cross section divided



into strips.

There is no specific value for the plastic moment in R/C because the moment capacity of the R/C cross section decreases continuously after reaching the ultimate moment of that section. The steel and confined concrete model are also employed together in the case of a cast in steel shell pile (CISS).

#### EMPLOYMENT OF THE NONLINEAR BEHAVIOR OF PILE MATERIAL IN THE STRAIN WEDGE MODEL ANALYSIS

As presented by Ashour et al. (1996 and 1998), the SW model parameters are related to an envisioned three-dimensional passive wedge of soil developing in front of the pile. The basic purpose of the SW model is to relate stress-strain-strength behavior of the layered soil in the wedge to one-dimensional Beam on Elastic Foundation (BEF) parameters in order to solve the following differential equation:

$$EI \frac{d^4 y}{d^4 x} + E_s(x)y + P_v \frac{d^2 y}{d^2 x} =$$

$$M \frac{d^2 y}{d^2 x} + E_s(x)y + P_v \frac{d^2 y}{d^2 x} = 0 \quad (9)$$

where

- M = Bending moment
- $P_v$  = Axial load
- y = Pile lateral deflection
- x = Location of pile section below pile head

The SW model is able to provide a theoretical link between the more complex three-dimensional soil-pile interaction and the simpler one-dimensional BEF characterization. The SW model links the nonlinear variation in the Young's modulus ( $E = \Delta\sigma_h/\epsilon$ , Fig. 6) of the soil to the nonlinear variation in the modulus of subgrade reaction ( $E_s = p/y$ , Fig. 7) associated with BEF characterization as illustrated in detail by Ashour et al. (1998).

As presented by Vesic (1961) and Francis (1964), the bending stiffness (EI) is one of the parameters which affects the modulus of subgrade reaction ( $E_s$ ). Ashour and Norris (2000) presented

a study, based on the SW Model, that showed the influence of the variation in the pile bending stiffness (EI) on the nature of the resulting p-y curve, assuming a constant elastic EI for the whole pile.

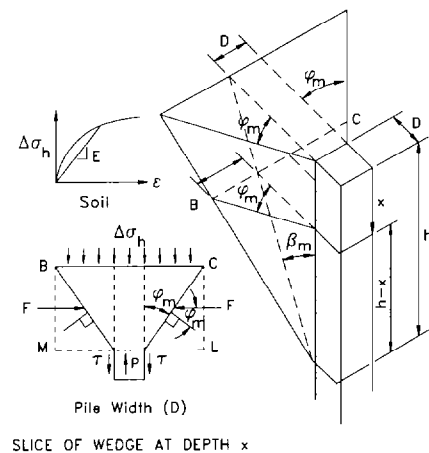


Fig. 6. Basic configuration of the strain wedge model (Ashour et al. 1998).

As seen by Eqn. 1, the response of the laterally loaded pile is a function of M and EI. Using nonlinear modeling for the strength of the pile material (concrete and/or steel) leads to a softer response (less Young's modulus, E, and/or a cracked R/C section which, in turn, means less moment of inertia, I) with increasing pile-head load and moment at a given depth. The SW Model has the capability to account for this reduction in EI on the response of the laterally loaded pile and the associated p-y curves.

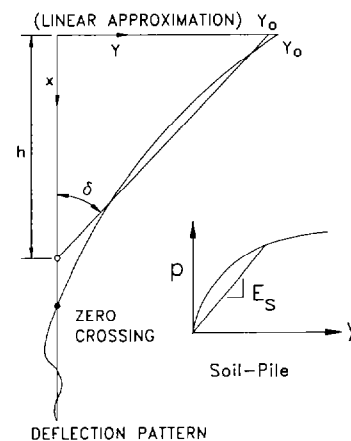


Fig. 7. Pile lateral deflection based on soil-pile properties (Ashour et al. 1998).

As derived and presented by Ashour et al. (1998) and shown by Eqn. 10, the variation in  $E_s$  with depth is a function of the geometrical shape (i.e. the size) of the developing and ever changing three-dimensional passive wedge of soil in front of the pile, the stress level (SL) in the soil (and the associated variation in soil E), and the corresponding deflection pattern of the loaded pile. This combination of soil and pile properties is presented in Eqn. 10.

$$(E_s)_i = \frac{p_i}{y_i} = \frac{A_i D \varepsilon E_i}{\delta (h - x_i)} = \frac{A_i}{(h - x_i)} D \Psi_s E_i \quad (10)$$

where  $i$  is the number of soil sublayer or pile segment;  $p$  and  $y$  are the soil-pile reaction and the pile's lateral deflection, respectively, at each pile segment. Soil parameter  $\Psi_s$  varies with the Poisson's ratio and stress level (SL) of the soil. Parameter  $A$  in the SW model links the BEF  $p$  to the horizontal stress change ( $\Delta\sigma_h$ ) in the soil at the face of the passive wedge (BC in Fig. 6) and is a function of both soil and pile properties (Ashour et al. 1998).  $h$  is the current depth of the mobilized passive wedge.

From Eqns. 9 and 10, it is obvious that any change in  $EI$  will have an impact on the lateral deflection ( $y$ ), the associated shape of the passive wedge ( $h, \delta$ , and  $\varphi_m$ ), and soil dependent parameters ( $E, \Psi_s$ , and  $A$ ), as seen in Figs. 6 and 7.

Using the nonlinear models for pile material presented above, the bending moment along the pile and the associated  $EI$  are calculated by iteration at each step. The solution procedure consists of calculating the value of bending moment ( $M_i$ ) at each cross section associated with a profile of the modulus of subgrade reaction ( $E_s$ ) which is induced by the applied load at the pile top. Then, the associated curvature ( $\phi$ ), stiffness ( $EI$ ), normal stress ( $\sigma_x$ ) and normal strain ( $\varepsilon_x$ ) can be obtained.

This procedure depends on the pile material. The profile of moment distribution along the deflected portion of the pile is modified in an iterative fashion along with the values of the strain, stress, stiffness and curvature to satisfy the equilibrium between the applied load and the associated responses of the soil and pile. This procedure guarantees the incorporation of soil-pile interaction with the material modeling. The technique presented strives for a more realistic assessment of the pile deflection pattern under lateral loading due to the nonlinear response of the pile material and the consequent soil resistance.

It should be noted that employment of pile/shaft material modeling is very important in predicting the ultimate capacity, lateral deflection, and the associated moment of the loaded pile/shaft. The simplified procedure of using a single  $EI$  of the cracked section could be used to predict the response of the laterally loaded pile/shaft, but with much less certainty. The influence of the variation in  $EI$  on the assessed  $p$ - $y$  curve will be obvious and especially significant over the zone of large bending moment. For the case of fixed-head conditions, the critical zone will be at the pile/shaft head, where a plastic hinge will develop reducing the pile's capacity.

The SW model has the capability of analyzing the behavior of the laterally loaded piles beyond the development of the first plastic hinge. The pile fails when pile stiffnesses at several sections (critical sections under large moment) drop to small values at which time the equilibrium between pile and soil resistances, and the external loads is not satisfied.

## CASE STUDIES / ILLUSTRATIVE EXAMPLES

### Paper No. 6.10

### Fixed-Head Drilled Shaft in Stiff Clay

As reported by Reese (1984) as an illustrative problem, a fixed-head drilled shaft of 30-inch outer diameter with 12 No. 8 rebars (steel area = 61.2 cm<sup>2</sup>) placed on a 0.6 m-diameter circle, was constructed in stiff clay. The ultimate strength of the concrete is assumed to be 27.5 MPa, and the yield strength of the steel is 420 MPa. The shaft exhibits an initial stiffness value ( $EI$ ) of  $5.4 \times 10^5$  kN-m<sup>2</sup> and is subjected to an axial load of 222 kN.

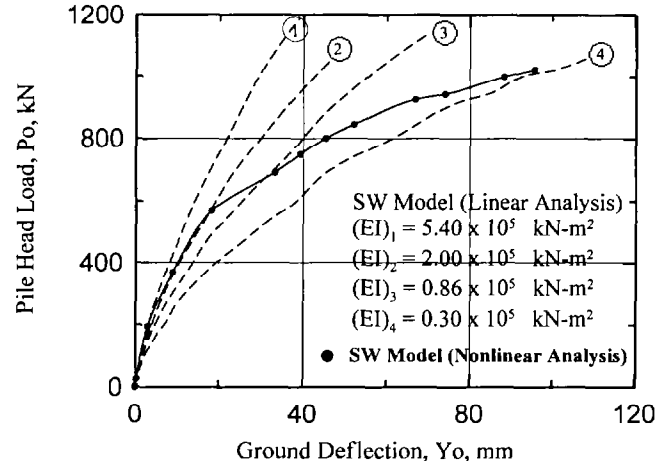


Fig. 8. Response of a laterally loaded fixed-head drilled shaft using material modeling.

The drilled shaft has been analyzed using the SW model considering different constant stiffness values (linear analysis). The assumed stiffness values range from the initial stiffness to a low stiffness of  $0.3 \times 10^7$  kN-m<sup>2</sup> which represents 5.5 percent of the initial stiffness. As seen in Fig. 8, the response of this laterally loaded fixed-head shaft assessed using the nonlinear SW material model intersects the curves for the constant stiffness values sequentially. The difference between the constant stiffness curve and the nonlinear material curve demonstrates the error involved in assuming a constant  $EI$  value, and secondly, the difficulty in picking an appropriate reduced value of  $EI$  to use in a linear analysis.

### Houston Test in Stiff Clay

A drilled shaft in stiff clay was tested under lateral loading at a site in Houston (Reese and Welch, 1975). The drilled shaft was 13 m long, 0.76 m in diameter, and had an initial  $EI$  of  $4.2 \times 10^5$  kN-m<sup>2</sup>. Difficulties encountered during pouring this free-head concrete shaft affected the value of  $EI$  and the measured data. Longitudinal and transverse steel reinforcement ratios in the SW

model analysis are assumed based on recommendations by Mander et al. (1988).

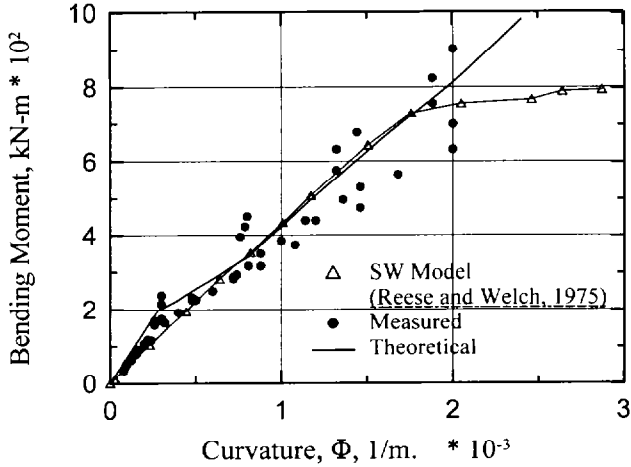


Fig. 9. Observed and calculated moment-curvature relationship for a tested drilled shaft.

Figure 9 shows a comparison between the measured and theoretical M- $\Phi$  relationship (Reese and Welch, 1975), and the values obtained by the SW model analysis using nonlinear models for steel and concrete. Failure in the concrete section induced by tensile stresses is predicted the upper portion of the the SW model results.

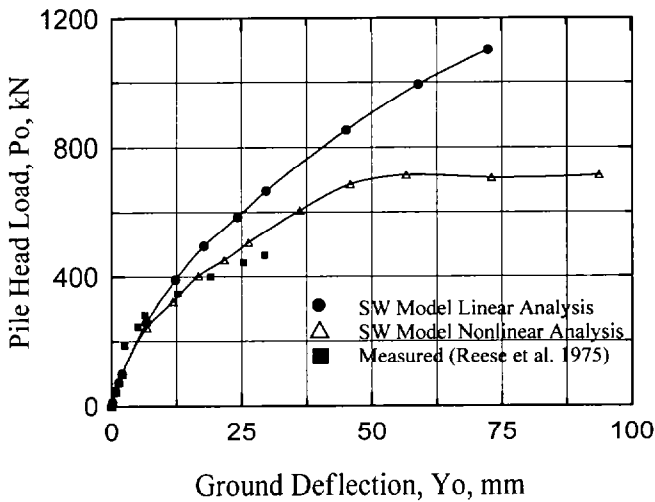


Fig. 10. A comparison of measured and predicted shaft-head response at Houston test.

Figure 10 provides a comparison between observed and predicted responses. Note the improved SW model capability provided by nonlinear material modeling.

As seen in Fig. 11, such nonlinear material behavior causes a change in p-y response, particularly in the zone of maximum moment. As expected, differences between linear and nonlinear model responses of Figs. 10 and 11 are small at the lower levels of load/deflection.

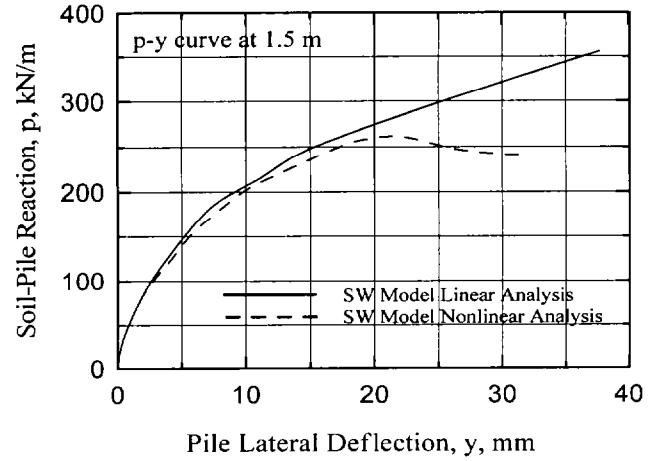


Fig. 11. Effect of nonlinear behavior of the drilled shaft material (R/C) on the nature of the p-y curve.

### Pyramid Building Test in Layered Clay

A lateral load test was performed on a full-scale pile in downtown Memphis. In order to improve the lateral capacity of the piles associated with this building, 1.8 meters of soft soil around the piles was removed and replaced with stiff compacted clay. The reported (unmodified) soil properties of the fill and the lower soil strata are presented by Reuss et al. (1992). The pile tested was a reinforced concrete pile of 0.40 m diameter, 22 m length, and 38742 kN-m<sup>2</sup> bending stiffness. In the SW model analysis, the ratio of longitudinal and transverse steel reinforcement of the pile is assumed to be 0.03 and 0.005, respectively.

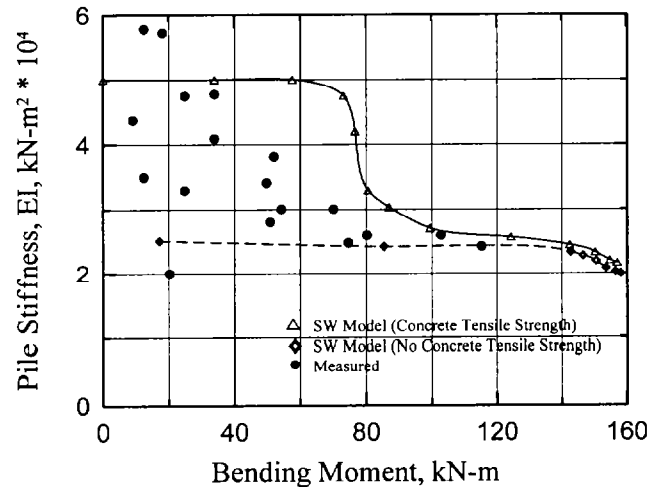


Fig. 12. Observed and predicted stiffnesses of the pile tested at Pyramid building site, Memphis, Tennessee.

Figure 12 provides a comparison between the measured and predicted M-EI relationship. The observed data falls between the predicted nonlinear curves obtained considering and neglecting the concrete tensile strength.

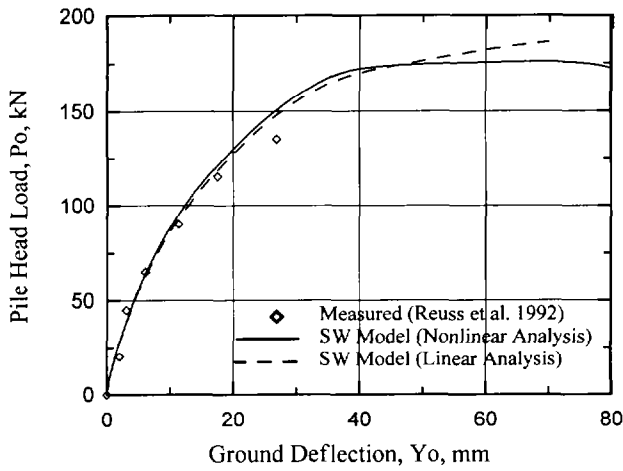


Fig. 13. Measured and Predicted lateral response of the R/C pile tested at the Pyramid building site.

The measured and predicted pile-head deflection versus lateral load is shown in Fig. 13. The pile experiences a limited (predicted) capacity at a lateral load of 175 kN. However, it is flow around failure of the clay rather than nonlinear material behavior that dictates response in this case. The effect of the nonlinear stiffness of the R/C pile on the soil-pile reaction (i.e. p-y curve) is exhibited in Fig. 14.

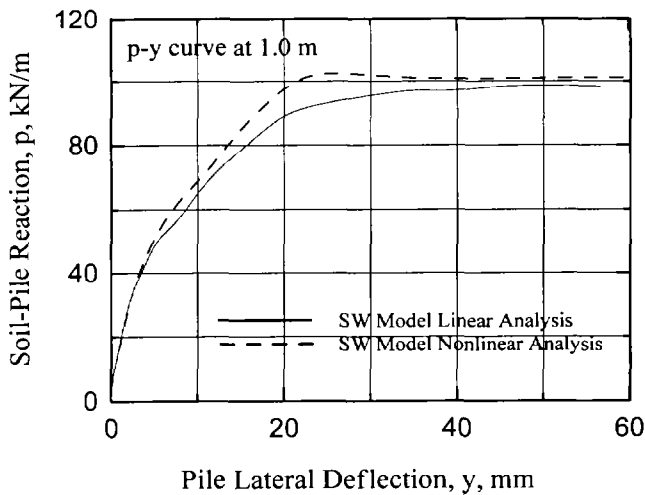


Fig. 14. Effect of nonlinear behavior of pile material (R/C) on the associated p-y curve at Pyramid Building Site.

Despite the significant effect of reduction in EI, the growth of the p-y curves ceases because of the flow around failure in the upper clay layer at this depth (Ashour and Norris, 2000). This particular field case demonstrates that depending on soil conditions, nonlinear material behavior may or may not have a significant influence on the resulting behavior. However, without the nonlinear analysis model, one would not know.

University of Texas, Austin, Test in Sand

The impact of the nonlinear behavior of steel on the response of

steel pipe piles is not seen until the outer fiber of the steel cross section reaches the yield stress. Figures 15 and 16 exhibit the response of a laterally loaded steel pipe pile driven into 2.9 m of sand layer underlain by a layer of stiff clay (Morrison and Reese, 1986).

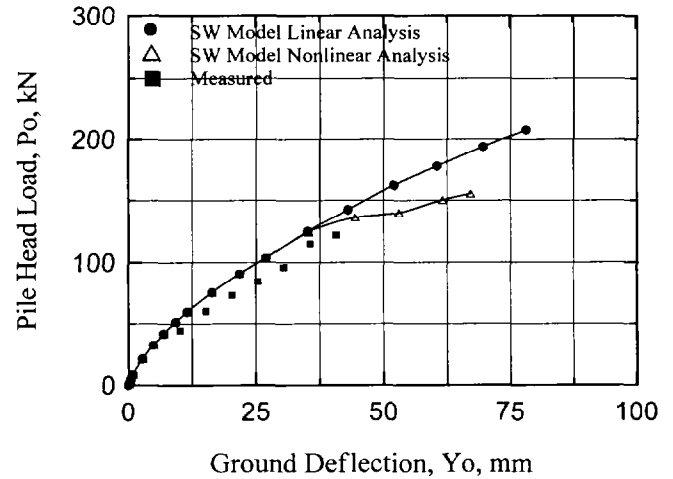


Fig. 15. Measured and predicted lateral response of a steel pile in sand (Morrison and Reese, 1986).

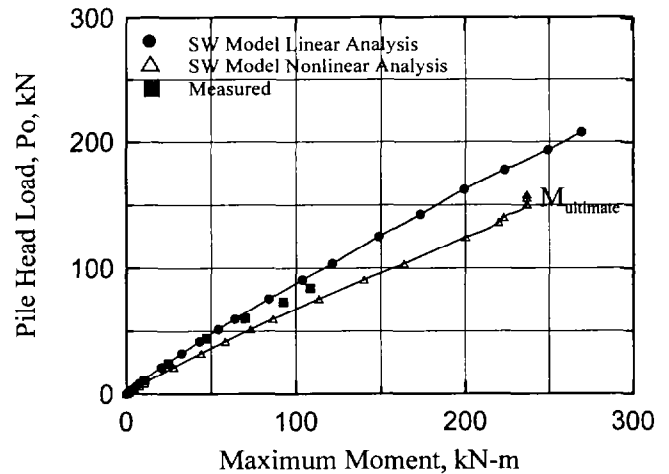


Fig. 16. Measured and predicted pile-head load vs. max. moment for a laterally loaded steel pile in sand (Morrison and Reese, 1986).

The data assessed using the SW model linear and nonlinear analyses are similar until the strains in the zone of maximum bending moment exceed the yield strain of the steel. Thereafter, the values of EI of cross sections in this zone decrease and start to affect the assessed nonlinear pile response (Figs. 15 and 16) and the associated p-y curves. As seen in Fig. 17, the p-y curve at this depth ceases to grow when the plastic hinge develops in the pile. The p-y curves outside the zone of the maximum bending moment are also affected, though not as much (based on the corresponding values of bending moment).



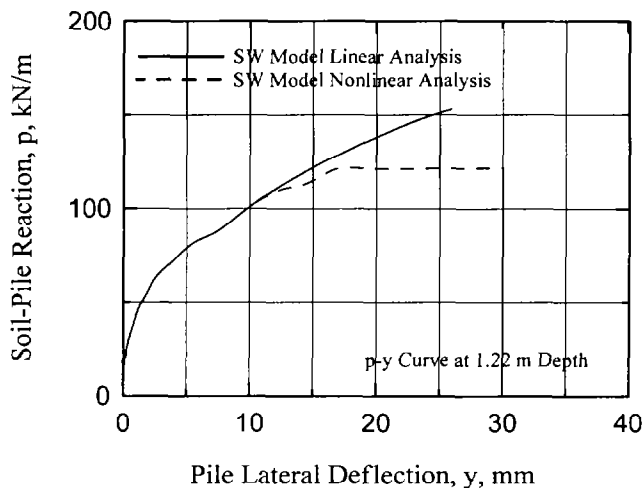


Fig. 17. Effect of nonlinear behavior of pile material (steel) on the associated  $p$ - $y$  curve and the ultimate value of soil-pile interaction.

## SUMMARY

The nonlinear behavior of the pile/shaft material has an influence on the lateral response and capacity of the pile/shaft. This effect is dependent on the values of bending moment (level of loading). In turn, the modulus of subgrade reaction (i.e. the  $p$ - $y$  curve) is affected by the changed bending moment, the reduced bending stiffnesses, and the changed deflection pattern of the pile/shaft. The nonlinear behavior of confined concrete has a significant impact on the nature of the  $p$ - $y$  curve, and the lateral capacity of concrete piles and drilled shafts. While, flow around failure in clay (which depends on pile bending stiffness) may limit the growth of the soil-pile reaction (i.e. the  $p$ - $y$  curve) before the nonlinear pile behavior affects it, the pile/shaft resistance is still affected by the degradation in bending stiffness. Without the appropriate implementation of material modeling, the pile/shaft capacity, and the associated deflection pattern and bending moment distribution will be difficult to predict with any degree of certainty.

## ACKNOWLEDGMENTS

This research was sponsored by the California Department of Transportation (CALTRANS) under Contract No. 59A0160. The authors would like to thank Mr. Steve McBride, Dr. Saad El-Azazy, and Mr. Tim Leahy for their interest and encouragement

## REFERENCES

- Ashour, M., Norris, G., and Pilling, P. [1998]. *Lateral Loading of a Pile in Layered Soil Using the Strain Wedge Model.* @ *Journal of Geotechnical and Geoenvironmental Engineering*, ASCE, Vol. 124, No. 4, April, 1998, pp. 303-315.
- Ashour, M. and Norris, G. [2000]. *Modeling Lateral Soil-Pile*

*Response Based on Soil-Pile Interaction.* @, *Journal of Geotechnical and Geoenvironmental Engineering*, ASCE, Vol. 126, No. 5, pp. 420-428.

Mander, J. B., Bristley, M. J. N., and Park, R. [1988]. *Theoretical Stress-Strain Model for Confined Concrete.* @, *Journal of Structural Engineering*, ASCE, Vol. 114, No. 8, pp. 1804-1826.

Morrison, C. and Reese, L. C. [1986]. *Lateral-Load Test of a Full-Scale Pile Group in Sand.* @, The Minerals Management Service, U. S. Department of Interior, Reston, Virginia; Department of Research, Federal Highway Administration, Washington, D. C.; U. S. Army Engineer, Waterways Experiment Station, Vicksburg, Mississippi, August.

Paulay, T., and Priestley, M. J. N. [1992]. *Seismic Design of Reinforced Concrete and Masonry.* @ John Wiley and Sons, New York, N.Y., pp. 95-157.

Reese, L. C. and Wang S. T. [1994]. *Analysis of piles under lateral loading with nonlinear flexural rigidity.* @ U.S. FHWA Int. Conf. On Design and Construction of Deep Foundation, FHWA, Washington, D.C.

Reese, L. C. [1984]. *Handbook on Design of Piles and Drilled Shafts under Lateral Load.* @ Geotechnical Engineering Center, Bureau of Engineering Research, University of Texas at Austin., Report No. FHWA-IP-84-11

Reese, L.C., and Welch, R. C. [1975]. *Lateral Loading of Deep Foundations in Stiff Clay.* @ *Journal of Geotechnical Engineering Division*, ASCE, Vol. 101, GT. 7, July, 1975.

Reuss, R., Wang, S. T., Reese, L. C. [1992]. *Tests of Piles Under Lateral Loading at the Pyramid Building, Memphis, Tennessee.* @ *Geotechnical News*, December, pp. 44-46.